Eur. Phys. J. C 28, 203–209 (2003)
Digital Object Identifier (DOI) 10.1140/epjc/s2003-01190-8

THE EUROPEAN PHYSICAL JOURNAL C

Anisotropic scintillators for WIMP direct detection: revisited

R. Bernabei[1], P. Belli[1], F. Nozzoli[1], A. Incicchitti[2]

[1] Dip. di Fisica, Universitá di Roma "Tor Vergata" and INFN, sez. Roma2, 00133 Rome, Italy
[2] Dip. di Fisica, Universitá di Roma "La Sapienza" and INFN, sez. Roma, 00185 Rome, Italy

Received: 21 October 2002 /
Published online: 14 April 2003 –

Abstract. The possibility to effectively exploit the directionality of the measured counting rate as a signature for WIMPs by using anisotropic scintillators is revisited and discussed in some details.

1 Introduction

Both cosmology and experimental observations have indicated the presence in the Galaxy of a dark matter halo, largely constituted of WIMPs (weakly interacting massive particles), relics from the big bang, non-relativistic at decoupling time. These particles can directly be detected deep underground by a suitable low radioactive experiment investigating their elastic scattering with the nuclei of the target-detector. Since they are embedded in the Galactic halo, their impinging direction is preferentially opposite to the direction of the Earth velocity in the Galaxy; thus, in principle, the direction of the recoiling nucleus can offer a model-independent signature for WIMPs [1], named *directionality signature* in the following. In fact, while the nuclear recoils induced by WIMPs are strongly correlated with the WIMPs' impinging direction, the background events obviously are not.

Low pressure TPCs have been suggested to detect WIMP induced recoils (see e.g. [2]), whose range is typically of order of μm in solid detectors; however, though unlikely, a realistic experiment would be limited, for example, by the necessity of a great operational stability, of a very large sensitive volume and of a great spatial resolution to reach a significant sensitivity. These practical limitations, which would affect possible experiments aiming to detect recoil tracks, can be overcome by using an alternative experimental approach based on the use of anisotropic scintillators as some of us firstly suggested in [3]; on this basis some preliminary activities have recently been carried out by various authors [4,5].

This idea is revisited in the present paper where both the approach and the related formulae are discussed considering new details as well as possible reachable sensitivities.

2 Anisotropic scintillators and expected signal counting rate

The peculiarity of an anisotropic scintillator, such as an anthracene and stilbene organic crystal, is the fact that its light response to heavy particles (p, α, recoil nuclei, $\cdots$) depends on their impinging direction with respect to the crystal axes. Such an anisotropic effect has been ascribed to preferred directions of the exciton propagation in the crystal lattice which affect the dynamics of the scintillation mechanism [6]. In particular, measurements performed in the past have shown that the light response of an anthracene scintillator to 6.56 MeV α particles impinging in the direction of the b-axis (a-axis) is 66% (80%) of the light response obtained when the same particles impinge in the direction of the c'-axis (where the light yield reaches its maximum value) [6] and that, in the measured energy range, these differences in the light response increase when decreasing the energy [6]. Moreover, it has also been verified that such an anisotropy is not present in case of electron excitation. Recently, the light response to proton recoils in a stilbene scintillator has been measured [5] to be in the range 0.10 to 0.17 for recoil energies between 300 keV and 3 MeV; moreover, these measurements have shown that the light response to proton recoils perpendicular to the cleavage plane is $\simeq$ 80% of the light response obtained for proton recoils parallel to the same plane [5]. Measurements of the quenching factor and of the anisotropic effect down to tens of keV have also been reported e.g. in [4], showing an effect still quite appreciable.

The features of the anisotropic scintillators could be exploited to investigate the WIMP component in the galactic halo. In fact, heavy ionizing particles with a preferred direction (like recoil nuclei induced by WIMP–nucleus elastic scattering) could, in principle, be discriminated from the electromagnetic background by comparing the low energy distributions measured by using different orientations of the crystal axes. Let us now quantitatively discuss the *directionality signature* by introducing the expected signal counting rate in case of the WIMP elastic scattering on the target-nuclei of an anisotropic scintillator.

Since the detectors are calibrated underground with gamma sources (see footnote 1 on the next page), a fundamental quantity in the calculation of the expected re-

coil energy distribution is the ratio of the light response to a recoil nucleus with respect to the light response to an electron having the same kinetic energy; this quantity is typically named the *quenching factor*. In the particular case of an anisotropic scintillator at rest in the laboratory frame having the coordinate axes coincident with the crystal axes, it can be written as

$$q_n(\Omega_{\rm out}) = q_{n,x}\sin\gamma\cos\phi + q_{n,y}\sin\gamma\sin\phi + q_{n,z}\cos\gamma, \quad (1)$$

where $q_{n,i}$ indicates the *quenching factor* value for a given nucleus (n) with respect to the ith axis of the anisotropic scintillator crystal; γ and ϕ are the polar and azimuthal angles for the outgoing direction of the nuclear recoil in the laboratory frame, and $\Omega_{\rm out}$ is the corresponding solid angle. This dependence of q_n on the anisotropic scintillator's axes induces a dependence also for the expected signal counting rate in the elastic scattering between a WIMP with mass $m_{\rm W}$ and a nucleus with mass m_n. Thus, the expected signal rate, R_n, will depend on the time since the detector is at rest in the laboratory frame and the orientations of the crystal axes vary with time because of the motion of the Earth. In particular, it can be written as

$$\frac{{\rm d}R_n}{{\rm d}E_{ee}}(E_{ee},t) = \int {\rm d}^3\mathbf{v}\,{\rm d}\Omega_{\rm cm} K\left[E_{ee} - q_n(\Omega_{\rm out})E_n\right] \times \frac{{\rm d}S_n}{{\rm d}\Omega_{\rm cm}\,{\rm d}^3\mathbf{v}}, \quad (2)$$

where (i) E_{ee} is the recoil energy in keV electron equivalent; (ii) $\mathbf{v}$ is the WIMP velocity in the laboratory frame; (iii) $\Omega_{\rm cm} = (\mu,\xi)$ is the nuclear recoil direction in the c.m. frame with μ the cosine of the scattering angle and ξ the corresponding azimuthal angle; (iv) $\Omega_{\rm out}$ is related to[2] $\Omega_{\rm in} = (\cos\alpha,\beta)$, which is the direction of the impinging WIMP in the laboratory frame, and to $\Omega_{\rm cm}$ by the expressions [1]

$$\cos\gamma = \sqrt{\frac{1-\mu}{2}}\cos\alpha - \sqrt{\frac{1+\mu}{2}}\sin\alpha\cos\xi,$$

$$\sin\gamma\cos\phi = \sqrt{\frac{1-\mu}{2}}\cos\beta\sin\alpha - \sqrt{\frac{1+\mu}{2}}(\sin\beta\sin\xi - \cos\alpha\cos\beta\cos\xi),$$

$$\sin\gamma\sin\phi = \sqrt{\frac{1-\mu}{2}}\sin\alpha\sin\beta + \sqrt{\frac{1+\mu}{2}}(\cos\beta\sin\xi + \cos\alpha\sin\beta\cos\xi);$$

(v)

$$E_n(\mu,\mathbf{v}) = \frac{1}{2}m_{\rm W}v^2\frac{4m_nm_{\rm W}}{(m_n+m_{\rm W})^2}\frac{1-\mu}{2}$$

is the kinetic energy in the laboratory frame of the nucleus; (vi)

$$\frac{{\rm d}S_n}{{\rm d}\Omega_{\rm cm}{\rm d}^3\mathbf{v}}$$

is the differential interaction rate for incoming WIMPs with velocity $\mathbf{v}$; (vii) $K\left[E_{ee} - q_n(\Omega_{\rm out})E_n\right]$ represents the detector response and accounts for its light yield; in particular, for an ideal detector K would simply be equal to the Dirac δ, while for a real detector with a finite energy resolution Δ (the *practical* case) one gets

$$K\left[E_{ee} - q_n(\Omega_{\rm out})E_n\right] = \frac{1}{\sqrt{2\pi}\Delta}{\rm e}^{-\frac{(E_{ee}-q_n(\Omega_{\rm out})E_n)^2}{2\Delta^2}}.$$

In addition, from the expression of the WIMPs' flux, ${\rm d}\Phi = \frac{\rho_0}{m_{\rm W}}|\mathbf{v}|f\left[\mathbf{v}+\mathbf{v}_{\rm d}(t)\right]{\rm d}^3\mathbf{v}$ (where ρ_0 is the local WIMP halo density, $f\left[\mathbf{v}+\mathbf{v}_{\rm d}(t)\right]$ is the WIMPs velocity distribution in the galactic rest frame and $\mathbf{v}_{\rm d}(t)$ is the detector velocity in this reference frame), one can calculate the expected interaction rate for each species of target-nucleus in a considered detector, ${\rm d}S_n$:

$${\rm d}S_n = \frac{\rho_0 N_n}{m_{\rm W}}|\mathbf{v}|f\left[\mathbf{v}+\mathbf{v}_{\rm d}\right]{\rm d}^3\mathbf{v}\frac{{\rm d}\sigma_n}{{\rm d}\Omega_{\rm cm}}{\rm d}\Omega_{\rm cm}, \quad (3)$$

with N_n the number of target-nuclei of the nth species per mass unit.

Finally, if the differential cross section in the c.m. frame is assumed to be isotropic, we have $\frac{{\rm d}\sigma_n}{{\rm d}\Omega_{\rm cm}} = \frac{\sigma_{0,n}}{4\pi}F_n^2(q^2)$, where (i) $\sigma_{0,n}$ is the point-like cross section; (ii) $F_n^2(q^2)$ is a form factor which accounts for the finite size of the nucleus; (iii) $q^2 = 2m_nE_n$; one gets integrating the relation (2) over an energy window ranging from E_1 to E_2

$$R_n(E_1,E_2,t) = \int {\rm d}^3\mathbf{v}\int {\rm d}\Omega_{\rm cm}\frac{\rho_0 N_n}{m_{\rm W}}|\mathbf{v}|f\left[\mathbf{v}+\mathbf{v}_{\rm d}(t)\right]\frac{\sigma_{0,n}}{4\pi}F_n^2\left(E_n\right) \times \frac{1}{2}\left[{\rm erf}\left(\frac{q_n(\Omega_{\rm out})E_n - E_1}{\sqrt{2}\Delta}\right) - {\rm erf}\left(\frac{q_n(\Omega_{\rm out})E_n - E_2}{\sqrt{2}\Delta}\right)\right], \quad (4)$$

where, as mentioned above, both E_n and $\Omega_{\rm out}$ are functions of $\mathbf{v}$ and of $\Omega_{\rm cm}$. In case of a multi-atomic species detector, the generalization of the formulas given above is straightforward.

3 Some general considerations on $\mathbf{v}_{\rm d}(t)$

Considering the crucial role played by $\mathbf{v}_{\rm d}(t)$ in the *directionality signature*, let us preliminarily devote this short section to its suitable evaluation.

The detector velocity in the Galactic rest frame can be expressed as: $\mathbf{v}_{\rm d}(t) = \mathbf{v}_{\rm rot} + \mathbf{v}_{\rm LSR} + \mathbf{v}_{\rm E}(t)$, where $\mathbf{v}_{\rm rot}$ is the rotational velocity of the Milky Way around its polar axis, $\mathbf{v}_{\rm LSR}$ is the solar system's velocity with respect to the Local Standard of Rest and $\mathbf{v}_{\rm E}(t)$ is the Earth's velocity around the Sun. The direction of the Sun's velocity

[1] The use of a neutron source in a low background installation is forbidden by the subsequent activation of the materials

[2] Here α is the polar angle in spherical coordinates which identifies the WIMP direction in the laboratory frame, and β is the corresponding azimuthal angle

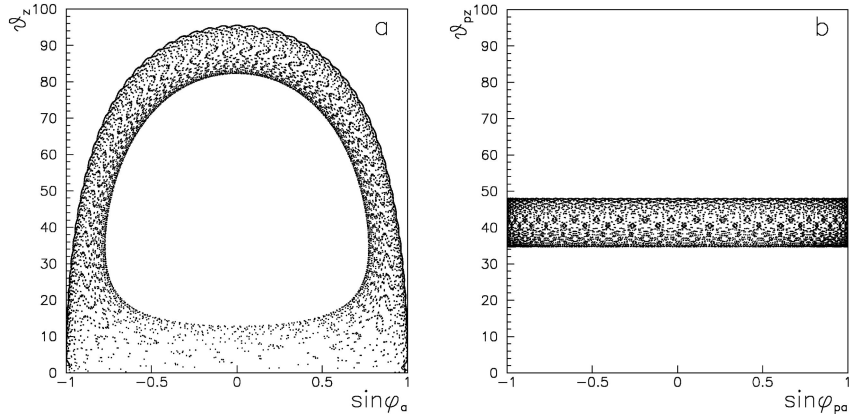

Fig. 1a,b. The various directions, in the sky, of the detector Galactic velocity $\mathbf{v}_{\rm d}(t)$ calculated for the next three years as viewed from LNGS (42°27′N latitude and 13°10′50″E longitude) in the local horizontal coordinate frame **a** and in the coordinate frame located to the North pole **b**. See text

($\mathbf{v}_{\rm rot}+\mathbf{v}_{\rm LSR}$) can be found from the equatorial coordinates of the Galactic Center (265.5°R.A.; −28°decl.) and of the Galactic North Pole (192.25°R.A.; 27.4°decl.); it identifies a point, P, in the celestial sphere with galactic equatorial coordinates of 315.8°R.A. and 49.6°decl. The NOVAS routines [7] allow one instead to calculate the Earth's motion around the Sun; the Earth's velocity identifies a point in the celestial sphere which has an annual variation with respect to P.

When instead a laboratory rest frame such as e.g. the azimuth–zenith horizontal frame is considered, the direction of $\mathbf{v}_{\rm d}(t)$ roughly describes in the sky a circular trajectory centered in the Earth polar axis because of the Earth's diurnal rotation, implying a large diurnal time dependence of the $\mathbf{v}_{\rm d}(t)$ direction. As an example, Fig. 1a shows the various directions in the sky (identified by the polar and azimuthal angles $\phi_a(t)$ and $\theta_z(t)$) of $\mathbf{v}_{\rm d}(t)$ calculated for the next three years as they would be observed at the Gran Sasso National Laboratory (LNGS) of I.N.F.N. (42°27′N latitude and 13°10′50″E longitude). However, it is much more convenient to consider instead an horizontal coordinate frame located at the North pole (described by the "polar-zenith", $\theta_{\rm pz}(t)$, and by the "polar-azimuth", $\phi_{\rm pa}(t)$); in fact, in this case the area in the sky of interest for the calculation of the signal rate is only a strip. This is well demonstrated by Fig. 1b, which is analogous to Fig. 1a, but exploits this latter useful coordinate frame. As it can be seen, in this reference frame the direction of the $|\mathbf{v}_{\rm d}(t)|$ is now confined in the strip: $0 < \phi_{\rm pa}(t) \leq 2\pi$, $34.5° \lesssim \theta_{\rm pz}(t) \lesssim 48.1°$. Every point in this strip represents the mean WIMP arrival direction at a certain t.

In the following discussion we will consider this latter more convenient reference frame.

4 The anthracene as a *directional* detector

The traditional anisotropic scintillators which were addressed in [3] are the anthracene, $C_{14}H_{10}$, and the stilbene, $C_{14}H_{12}$, ones. The latter can offer in addition the possibility of a pulse shape analysis of the events, but it would require a higher energy threshold because of its lower light response. Thus, in the following we again prefer to discuss as a practical example the case of the anthracene scintillator (one could analogously proceed in the other case). In particular, in this case the expected number of photoelectrons/keV is 3 considering that the light response of an anthracene scintillator is about 17000 photons/MeV; thus, a threshold of about 2 keV can – in principle – be reached.

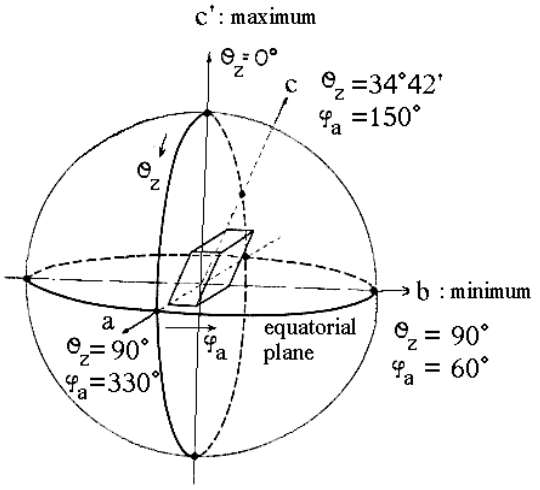

Fig. 2. A schematic representation of the crystal axes of anthracene. The *quenching factor* is maximal in the direction of the c'-axis, which is perpendicular to the ab plane [8]

A schematic representation of the anthracene crystal's axes is given in Fig. 2. Since the "polar-zenith" angle, $\theta_{\rm pz}$, is always near 40°, at a certain time of the day (generally in the morning at LNGS) the WIMPs come mainly from the top, while 12 h later they come near the horizon and from North (see Fig. 3). Thus, if a scintillator with an anisotropic light yield is considered, a suitable arrangement for such an experiment is to install the setup with the detectors' axis having the largest *quenching factor* value (the c'-axis in anthracene) in the vertical direction, and with the axis having the smallest *quenching factor* value (the b-axis in anthracene) towards the North. In this way, the behavior of the energy spectrum of the WIMP induced nuclear recoils diurnally varies and, therefore, also the counting rate. In practice, the investigation can be performed as a function of $\mathbf{v}_{\rm d}(t)$.

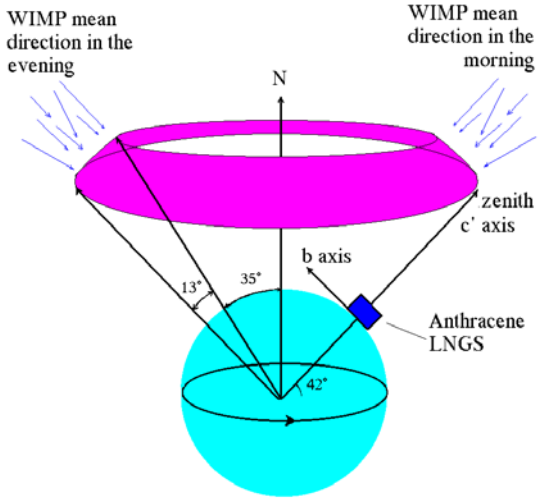

Fig. 3. Schematic representation of the experimental approach mentioned in the text. The anthracene detector is placed ideally at LNGS with the c'-axis in the vertical direction and the b-axis pointing to the North. The area in the sky from which the WIMPs are preferentially expected is highlighted

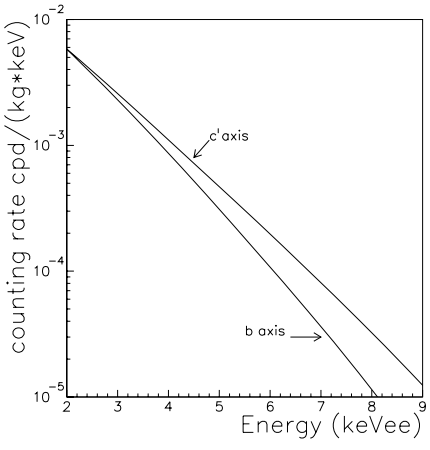

Fig. 4. Example of the expected signal counting rate of WIMP induced nuclear recoil in an anthracene detector for a WIMP flux mainly impinging along the c'-axis and along the b-axis, respectively. In this example the WIMP mass has been assumed to be 50 GeV, the WIMP–proton cross section to be $3 \cdot 10^{-6}$ pb and the model framework to be the one given in the text

In the following, to perform the calculations needed to investigate the features of a possible experiment with anthracene detectors, the *quenching factor* values for the c'-axis $q_{H,c'} = 0.2$ and $q_{C,c'} = 0.1$ have been considered, as well as the ratios $\frac{q_{c'}}{q_a} = 1.23$ and $\frac{q_{c'}}{q_b} = 1.52$ (these latter ones have been assumed equal for the two atomic species) [6].

At this point, a model framework has also to be fixed; this is identified not only by general astrophysical, nuclear and particle physics assumptions, but also by the set of parameter values (such as WIMP local velocity, v_0, form factor parameters, etc.) used in the calculations. In the following, for simplicity, we will follow a frequently considered simplified approach fixing a set of assumptions and of values, without considering the large effect of the existing uncertainties on each one of them; obviously, the reader should keep in mind the large uncertainties consequently associated to the presented results.

We preliminarily note that the contribution to the differential energy spectrum due to WIMP–hydrogen elastic scattering is negligible because of the relative small mass of the hydrogen nuclei. This implies also that the organic scintillators are substantially non-sensitive to spin-dependent (SD) coupled WIMPs since natural C has only 1.11% of odd spin isotopes. Therefore, in the following only the particular case of WIMPs with dominant spin-independent (SI) coupling will be considered. The results will be given in terms of the WIMP elastic cross section on a proton, σ_p, assuming for the scaling law from the WIMP–carbon elastic cross section, $\sigma_{\rm C}$, the following relation:

$$\sigma_{\rm C} = \sigma_p \left(\frac{M_{\rm C}^{\rm red}}{M_p^{\rm red}} \cdot A \right)^2 = \sigma_p \left(\frac{m_p + m_{\rm W}}{m_{\rm C} + m_{\rm W}} \cdot \frac{m_{\rm C}}{m_p} \cdot A \right)^2 . \quad (5)$$

Here $M_{\rm C}^{\rm red}$ ($M_p^{\rm red}$) is the reduced mass of the carbon (proton)–WIMP system. Moreover, for simplicity we will assume here e.g. (i) a simple exponential form factor: $F_n^2(E_n) = {\rm e}^{-\frac{E_n}{E_0}}$ with $E_0 = \frac{3(\hbar c)^2}{2 m_n r_0^2}$ and $r_0 = 0.3 + 0.91 \sqrt[3]{m_n}$ (r_0 is the radius of the nucleus in fm when m_n is in GeV); (ii) a simple spherical isothermal WIMP halo model[3], giving

$$f(\mathbf{v}_{\rm g}) = \frac{1}{\pi^{3/2} v_0^3} {\rm e}^{-\frac{|\mathbf{v}_{\rm g}|^2}{v_0^2}} \Theta(v_{\rm esc} - |\mathbf{v}_{\rm g}|),$$

where $v_{\rm esc}$ is the escape velocity of the Galaxy (here assumed equal to 650 km/s), v_0 is the WIMP local velocity (here assumed to be equal to 220 km/s) and $\mathbf{v}_{\rm g}$ is the WIMP velocity in the Galactic rest frame; Θ is the Heaviside function.

For this given model framework the signal counting rate expected in an anthracene detector, considering alternatively the cases of c'-axis and b-axis parallel to the Earth velocity, has been calculated as an example for a WIMP with $m_{\rm W} = 50$ GeV and $\sigma_p = 3 \cdot 10^{-6}$ pb; it is shown in Fig. 4. Since the number of particles is a constant, the two energy distributions have a cross point; for this reason, depending on the considered energy window, the effect which allows one to point out a variation of the counting rate with respect to the crystal orientation can be positive, negative or – unluckily – null. This points out the general relevance of considering the differential energy spectrum in the data analysis.

[3] We recall that the spherical isothermal halo model – generally considered in this field – cannot be the correct one since it implies both a singularity in the center of the Galaxy and an infinite mass. More refined models exist, like those discussed e.g. in [11]. Obviously, the use of a more realistic halo model will modify the results; nevertheless considering this as a tutorial discussion, we maintain here this simplified description

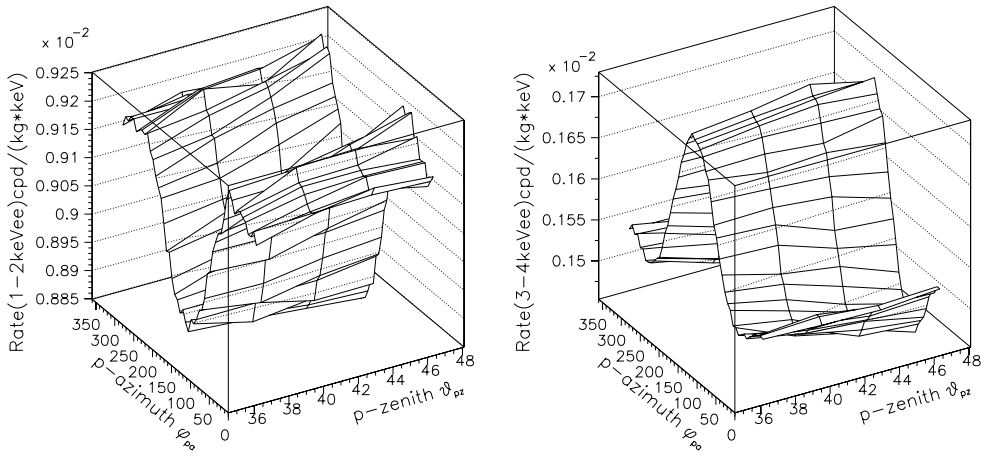

Fig. 5. Example of the expected rate, in the 1–2 keV and 3–4 keV energy windows, versus the detector's (or Earth's) possible velocity directions. As in Fig. 4, this example refers to the particular case of a WIMP mass assumed to be equal to 50 GeV, a WIMP–proton cross section assumed to be equal to $3 \cdot 10^{-6}$ pb and a model framework assumed to be as given in the text. As previously explained, there is a strong dependence on the "polar-azimuth" ($\phi_{\rm pa}$) that induces a diurnal variation of the rate

5 Reachable sensitivities

On the basis of the model framework given above, we have calculated for some cases the effect achievable when exploiting the WIMPs' *directionality signature* by the present approach using the schematic configuration of Fig. 3. The result is shown in Fig. 5, where an example of the dependence of the expected rate on the WIMP arrival direction with respect to the crystal axes is given; a clear dependence on $\phi_{\rm pa}$ (which gives the observed rate of diurnal variation because of the Earth's daily rotation) is present. In particular, the behaviors expected in the 1-2 keV and in the 3-4 keV energy windows are depicted there for the considered case; they show opposite signs of the rate variation amplitude than the possible case mentioned above.

We comment that convenient parameters for the data analysis are the amplitude of the diurnal rate variation, A_m, whose absolute value is defined as the semi-difference between the maximum and the minimum rate value, and the mean value of the rate, A_0, in the considered energy window.

This WIMP *directionality signature* is potentially very effective; however, in the practical realization we have suggested here, the effect's results are of the same order of magnitude as the one induced by the WIMP *annual modulation signature* based on the annual rate modulation induced by the Earth revolution around the Sun [10,11]. In Fig. 6a the absolute value of A_m is superimposed on the amplitude of the *annual modulation signature*, both calculated, as an example, again assuming a WIMP mass equal to 50 GeV, a WIMP–proton cross section equal to $\sigma_p = 3 \cdot 10^{-6}$ pb and the model framework and experimental features given above. In Fig. 6b the energy behaviors of the ratio $R = A_m/A_0$, for four WIMP mass values are shown. In the range of a few keV the variation of the rate due to the *directionality signature* is about 10%; it increases at higher energy, but the absolute value of the rate significantly decreases as well.

Let us now give an indicative evaluation of the sensitivity achievable when the *signal over noise ratio* is larger than n_σ (with n_σ equal to the required number of standard deviation for the signal; in the following, the considered confidence level is 90%) by means of the following relation between σ_p and $m_{\rm W}$ (through A_m and A_0):

$$A_m(\sigma_p, m_{\rm W}) > n_\sigma \sqrt{\frac{2 \cdot [A_0(\sigma_p, m_{\rm W}) + b]}{M_T \cdot T \cdot \Delta E}}. \qquad (6)$$

Here (i) ΔE is the considered energy window; (ii) $M_{\rm T}$ is the anthracene target-detector mass; (iii) T is the running time; (iv) b is the time-independent background[4]. In the following calculations they are assumed to be $M_{\rm T} = 500$ kg, $T = 10$ y and $b = 10^{-4}$ cpd/kg/keV. Moreover, the calculations are performed in the given model framework by considering bins of 1 keV up to 10 keV and two different energy thresholds. A typical energy resolution, $\sigma/E = \frac{0.9}{\sqrt{E[\rm keV]}}$, has been used. The regions explorable (at 90% C.L.) by the *directionality signature* for the given model framework are shown in Fig. 7a. However, although relatively good sensitivities are reported in Fig. 7a, the feasibility of such an experiment would present several practical difficulties requiring the use of a very large number of small anthracene detectors as well as the necessity of a new special development to create efficient, small size, high gain, highly radiopure scintillation light collector devices. Thus, it appears more suitable to pursue new

[4] For the sake of completeness, we mention that the DAMA low background Ge detector has measured deep underground in the Gran Sasso National Laboratory of I.N.F.N. the residual standard radioactive contaminants in a commercial anthracene crystal. The obtained results are limits at 95% C.L.: < 30 ppb of ^{238}U, < 7 ppm of $^{\rm nat}$K, $< 3.7 \cdot 10^{-10}$ ppb of ^{60}Co. Thus, this can be considered the present starting point for low background developments. Obviously, to reach a well reduced background level, the ^{14}C residual contamination at least at the level of the requirements of the Borexino experiment [9] would be necessary

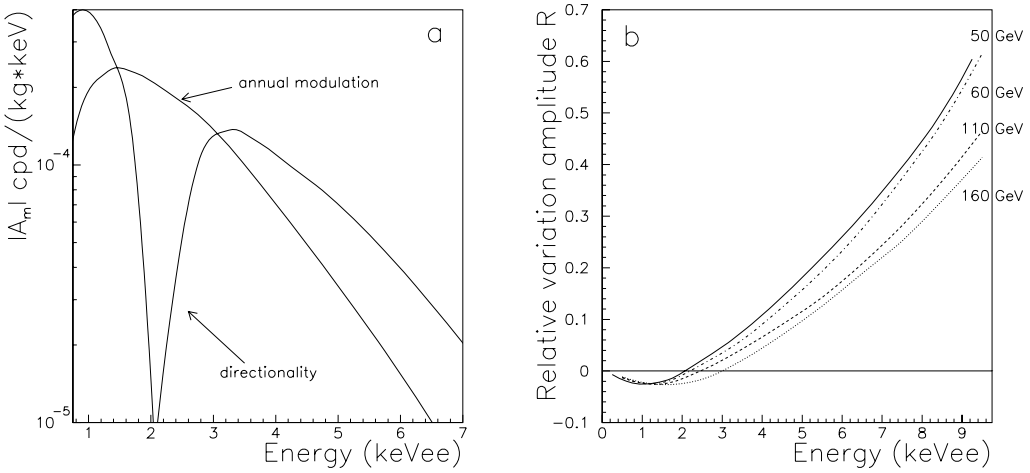

Fig. 6. a Example of the comparison between the rate of the diurnal variation induced in an anthracene detector by WIMP flux directionality and the corresponding annual modulation effect in the particular case of a WIMP mass assumed to be equal to 50 GeV, a WIMP–proton cross section assumed to be equal to $3 \cdot 10^{-6}$ pb and of the model framework given in the text. In this experimental realization the magnitude of the two signatures would be similar. **b** Energy behaviors of the relative variation amplitude R (see text) for various $m_{\rm W}$; the large value of R at higher energy is not useful in practice because of the significant decreasing of the A_m and A_0 values

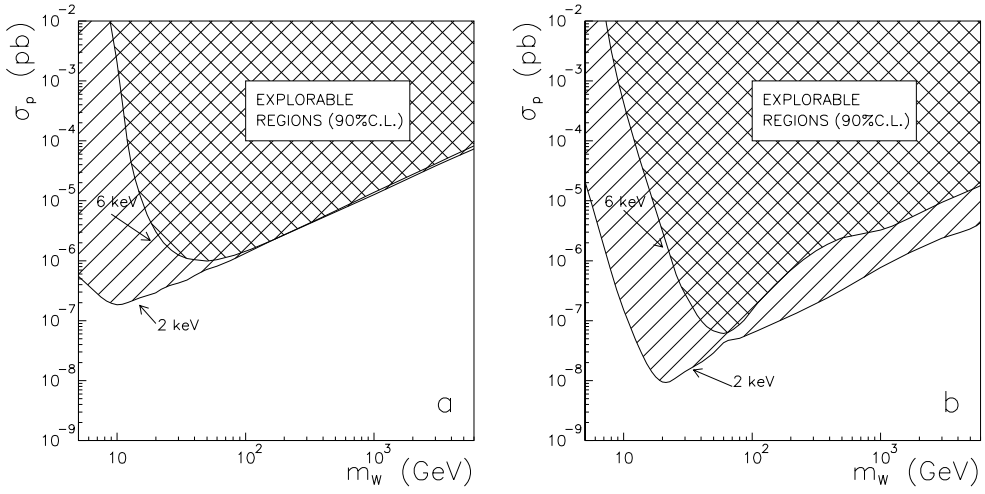

Fig. 7. Sensitivity (90% C.L.) reachable with the *directionality signature* in 10 y of running – provided a time-independent background $b = 10^{-4}$ cpd/kg/keV and a SI coupled WIMP – for 2 and 6 keV energy thresholds in the simplified model framework given in the text when **a** using 500 kg of anthracene; **b** using 500 kg of an hypothetical high atomic weight ($A = 140$) anisotropic scintillator; the interest in trying to develop a high A anisotropic scintillator is evident. In this way, the DAMA/NaI model-independent annual modulation evidence for a WIMP component in the Galactic halo [10,11] could be further investigated for the particular case of a purely SI coupled WIMP. We recall that a SI candidate with mass up to $\simeq 270$ GeV and cross section on a proton down to $\simeq 10^{-7}$ pb (given the assumed scaling laws, form factors and parameter values) is allowed by the DAMA/NaI data when accounting for different possible Galactic halo models [11]; a further extension is expected when accounting for the other existing uncertainties on astrophysical, nuclear and particle physics assumptions and parameters

devoted R&D's to develop anisotropic scintillators having significantly larger sizes, higher light responses, higher atomic weights and anisotropy features similar to or better than those of the anthracene scintillator. In case of success, the improvement in sensitivity shown in Fig. 7b could be reached (the energy resolution has been assumed there, for simplicity, equal to that of the anthracene case and the atomic weight, A, equal to 140)[5]. Thus, preliminary experimental efforts to develop new anisotropic scintillators are under consideration. Moreover, we also note that – in principle – a similar set-up could allow one to explore two distinctive signatures for WIMPs: the *annual modulation* [10,11] and the *directionality signatures* [1,3], offering an obviously increased sensitivity when they are at the same time exploited by a suitable likelihood analysis of the experimental data. This could allow one to

[5] We note that the shape of the sensitivity curves given in Fig. 7 depends on the lack of sensitivity already shown in Fig. 6 for a single 1 keV bin, which is however partially recovered by the contributions arising from the nearer bins

further investigate the nature of the WIMP candidate for the DAMA/NaI WIMP model-independent annual modulation evidence [10,11] at least for some model frameworks and a WIMP interaction type.

6 Conclusion

In this paper the possibility to exploit the *directionality* of the measured counting rate as a signature for WIMPs by using anisotropic scintillators – as we firstly suggested in [3] – has been revisited. Emphasis has been given to the methodological approach and reachable sensitivities in a particular given model framework. Technical difficulties and interests for devoted R&D have been mentioned.

References

1. D.N. Spergel, Phys. Rev. D **37**, 1353 (1988)
2. M.J. Lehner et al., astro-ph/9905074
3. P. Belli, R. Bernabei, A. Incicchitti, D. Prosperi, Il Nuovo Cim. C **15**, 475 (1992)
4. N.J.C. Spooner et al., International Workshop on Identification of Dark Matter (World Scientific 1997), p. 481
5. Y. Shimizu, M. Minowa, H. Sekiya, Y. Inoue, Nucl. Instr. and Meth. A **496**, 347 (2003)
6. J.B. Birks, The theory and practice of scintillation counting (Pergamon Press, London 1976); P.H. Heckmann, Z. Phys. **157**, 10 (1959); P.H. Heckmann, H. Hansen, A. Flammersfeld, Z. Phys. **162**, 84 (1961); W.F. Kienzle, A. Flammersfeld, Z. Phys. **165**, 1 (1961); K. Tsukada, S. Kikuchi, Nucl. Inst. and Meth. **17**, 286 (1962); K. Tsukada, S. Kikuchi, Y. Miygawa, Nucl. Inst. and Meth. **37**, 69 (1965); F.J. Kratochwill, Z. Phys. **234**, 74 (1970); F.D. Brooks, D.T. Jones, Nucl. Inst. and Meth. **121**, 69 (1974)
7. http://aa.usno.navy.mil/software/novas/
8. K. Tsukada, S. Kikuchi, Nucl. Inst. and Meth. **17**, 286 (1962)
9. Borexino Coll., Astrop. Phys. **18**, 1 (2002)
10. R. Bernabei et al., Phys. Lett. B **389**, 757 (1996); R. Bernabei et al., Phys. Lett. B **424**, 195 (1998); R. Bernabei et al., Il Nuovo Cimento A **112**, 545 (1999); R. Bernabei et al., Phys. Lett. B **450**, 448 (1999); P. Belli et al., Phys. Rev. D **61**, 023512 (1999); R. Bernabei et al., Phys. Lett. B **480**, 23 (2000); R. Bernabei et al., Eur. Phys. J. C **18**, 283 (2000); R. Bernabei et al., Phys. Lett. B **509**, 197 (2001); R. Bernabei et al., Eur. Phys. J. C **23**, 61 (2002)
11. P. Belli et al., Phys. Rev. D **66**, 043503 (2002)